Rapid Refolding of Native Epitopes on the Surface of Cytochrome *c*†

Michael J. Allen,‡ Ronald Jemmerson,§ and Barry T. Nall*,‡

Department of Biochemistry, University of Texas Health Science Center, San Antonio, Texas 78284-7760, and Department of Microbiology, University of Minnesota, Minneapolis, Minnesota 55455-0312

Received July 19, 1993; Revised Manuscript Received December 21, 1993®

ABSTRACT: Refolding of surface epitopes on horse cytochrome *c* has been measured by monoclonal antibody binding. Two antibodies were used to probe re-formation of nativelike surface structure: one antibody (2B5) binds to native cytochrome *c* near a type II turn (residue 44) while the other (5F8) binds to a different epitope on the opposite face of the protein near the amino terminus of an α-helical segment (residue 60). The results show that within the first ~100 ms of refolding all of the unfolded protein collapses to nativelike folding intermediates that contain both antibody binding sites. All three absorbance/fluorescence-detected kinetic phases in the folding of cytochrome *c* ($k_1 \sim 5\ s^{-1}$, $k_2 \sim 0.4\ s^{-1}$, $k_3 \sim 0.03\ s^{-1}$) are slower than the rates of re-formation of the antibody binding sites ($k_{obs} > 10.0\ s^{-1}$), suggesting that the formation of antibody binding sites precedes the refolding reactions observed in kinetically resolved optically-detected refolding phases. Kinetically unresolved folding processes account for 79% and 19% of the total fluorescence change and absorbance change, respectively, observed in equilibrium unfolding. Thus, kinetically unresolved folding reactions appear to be responsible for re-formation of the MAb binding sites within partially folded intermediate species. These species are nonnative (incompletely folded) in that their optical properties are in between those of the unfolded and the fully folded protein. As a test of whether antibody binding to folding intermediate(s) perturbs further folding, the rate of the absorbance-detected slow refolding phase has been measured for folding intermediate(s) of cytochrome *c* complexed with antibodies. Neither antibody had a significant effect on the rate of the absorbance-detected slow folding reaction, suggesting that changes in protein conformation associated with the absorbance-detected slow folding phase are not affected by possible antibody-induced changes in structure or stabilization of the epitopes. Since epitopes of protein antigens cover an extensive surface area (700–800 Å^2), the results show the major aspects of the nativelike surface topography are formed early (<100 ms) in folding intermediates.

Analysis of the structure of protein folding intermediates is an especially challenging problem. Experimental strategies for characterizing these species must take into account the transient nature of folding intermediates and, thus, be capable of obtaining detailed structural information on the millisecond to second time scale of the folding reactions. There are at least two methods capable of providing detailed information about the structure of folding intermediates. Both methods rely on rapid mixing techniques (stopped-flow mixing) but differ in methodology and in the type of structure detected. One method uses amide proton exchange to detect the formation of H-bonds. The other uses monoclonal antibody (MAb)[1] binding to monitor re-formation of native surface contours (epitopes) as the protein refolds. Thus, the application of both methods to the same protein should provide highly complementary structural information, although this has not yet been attempted for any protein. The proton exchange method, pioneered by Baldwin, Roder, Englander, and their colleagues (Baldwin & Roder, 1991; Roder et al., 1988; Roder & Wuthrich, 1986; Udgaonkar & Baldwin, 1988), involves deuterium pulse labeling of accessible amide proton sites in folding intermediates. The proton occupancy of samples labeled at different times after the initiation of refolding is assayed by 2D NMR spectroscopy. Since H-bonding protects against proton exchange, the pulse labeling method provides information on the time course of H-bond formation as the protein folds. Antibody-detected folding, pioneered by Goldberg and colleagues (Blond-Elguindi & Goldberg, 1990; Murry-Brelier & Goldberg, 1988), uses fluorescence changes upon antibody–antigen complex formation to measure the time course of appearance of protein epitopes during refolding. The folding of horse cytochrome *c* has been characterized previously by amide proton exchange pulse labeling (Roder et al., 1988) but not by monoclonal antibody binding. With the intention of providing a more complete picture of the structure of intermediates in folding of horse cytochrome *c*, we have used two distinct monoclonal antibodies to monitor refolding. The 2B5 MAb binds cytochrome *c* near a type II turn (residue 44) while the 5F8 MAb binds to a distinct epitope near the amino terminus of an α-helical segment (Goshorn et al., 1991). Both MAbs are known to have diffusion-limited rates of binding to native cytochrome *c* (Raman et al., 1992).

MATERIALS AND METHODS

Preparation of Protein Samples. The purification of type IV horse heart cytochrome *c*, and antibodies 5F8 and 2B5, and preparation of Fab fragments have been described (Raman et al., 1992). To ensure that the cytochrome *c* was fully

† Supported by National Institute of General Medical Sciences Grant GM32980 (B.T.N.), Robert A. Welch Foundation Grant AQ838 (B.T.N.), and National Science Foundation Grant DMB-9019181 (R.J.).

* Address correspondence to this author at the Department of Biochemistry, University of Texas Health Science Center, 7703 Floyd Curl Dr., San Antonio, TX 78284-7760.

‡ University of Texas Health Science Center.

§ University of Minnesota.

® Abstract published in *Advance ACS Abstracts,* March 15, 1994.

[1] Abbreviations: MAb, monoclonal antibody; Fab, antigen binding fragment of an MAb; nm, nanometers; μm, micrometers; mm, millimeters; μg, micrograms; DTT, dithiothreitol; SDS, sodium dodecyl sulfate; β-ME, β-mercaptoethanol; Gdn·HCl, guanidine hydrochloride; SDS–PAGE, polyacrylamide gel electrophoresis in the presence of sodium dodecyl sulfate; CD, circular dichroism.

0006-2960/94/0433-3967$04.50/0

oxidized, a slight molar excess of potassium ferricyanide was added to the cytochrome *c* solution and the ferricyanide removed by G-25 Sephadex chromatography. Apocytochrome *c* was prepared from horse heart cytochrome *c* by the procedure of Stellwagen et al. (1972). Silver sulfate (80 mg) was added to 9 mL of water and 0.8 mL of glacial acetic acid. Fifty milligrams of cytochrome *c* dissolved in 1 mL of water was added to the silver sulfate solution and incubated 5 h in the dark at 40 °C with gentle agitation. The apocytochrome *c* was passed through a G-25 Sephadex column equilibrated with 0.1 N acetic acid, lyophilized, and stored at −20 °C.

Immunoassays (ELISAs). Horse heart cytochrome *c* at 0.02 or 0.007 mg/mL as well as apocytochrome *c* at 0.02 mg/mL was adsorbed to separate wells of 96-well plates (Falcon) by overnight incubation of 0.05 mL of the proteins in 0.1 M sodium phosphate, pH 7.0, 4 °C. Excess adsorption sites were blocked by incubation with 1% bovine serum albumin (BSA) in sodium phosphate buffer (300 μL/well, room temperature) for 30 min. The wells were washed 3 times with sodium phosphate buffer/0.05% Tween-20 (wash buffer). Antibody supernatants (0.05 mL/well) were added and incubated for 2 h followed by three rinses with the wash buffer. Goat anti-mouse IgG conjugated to alkaline phosphatase (Bio-Rad) was diluted 1/6000 in the BSA buffer (1% BSA/0.1 M sodium phosphate, pH 7.0) and 0.05 mL added to each well. The plates were incubated at room temperature for 2 h. The wells were rinsed 6 times with the wash buffer [0.1 M sodium phosphate (pH 7.0)/0.05% Tween-20], and 0.05 mL of phosphatase substrate solution (Bio-Rad) was added to each well. After 30 min, the reaction was stopped by the addition of 0.05 mL of 1 M NaOH to each well. Absorbance measurements at 405 nm were recorded on a TiterTek ELISA plate reader.

For the 2B5 MAb, competition ELISAs were performed to verify that the lack of MAb–apocytochrome *c* binding was not a result of epitope disruption on binding to the ELISA plate. For these experiments, the plates were coated with 1 μM native cytochrome *c*. Two solutions were prepared in which 2B5 MAb was mixed with apocytochrome *c* at final concentrations of 2 μM MAb binding sites and 5 and 10 μM apocytochrome *c*. The solutions were incubated for 15 min at room temperature. The MAb–apocytochrome *c* solutions were added to the ELISA wells and incubated for an additional 15 min before the wells were rinsed and the ELISA plate was developed (described above). Three controls were performed: addition of MAb alone to the wells at a concentration of 2 μM binding sites; addition of 0.1 M sodium phosphate, pH 7, to the wells; and addition of preformed 2B5 MAb–cytochrome *c* complex to the wells at concentrations of 5 μM cytochrome *c* and 2 μM MAb binding sites. As with the MAb–apocytochrome *c* solutions, the control solutions were incubated 15 min in the wells before the wells were rinsed and the ELISA plate was developed. Controls gave the expected results. MAb alone gave a full ELISA response showing that 2B5 MAb binds tightly to horse cytochrome *c*. Neither the buffer alone nor the 2B5 MAb complexed with cytochrome *c* showed MAb binding. Both of the MAb solutions containing different concentrations of apocytochrome *c* showed full MAb binding to the plate, indicating that apocytochrome *c* does not inhibit 2B5 MAb binding to native cytochrome *c*. Apocytochrome *c* has limited solubility, especially in 0.1 M sodium phosphate buffer. The lyophilized apoprotein was dissolved as a 160 μM stock solution in 0.1 M acetic acid. The apoprotein stock was diluted by 32-fold and 16-fold into the 0.1 M sodium phosphate buffer, pH 7, to give final concentrations of 5 and 10 μM. Attempts to prepare more concentrated solutions of apoprotein in phosphate buffer gave precipitates.

Kinetic Experiments. All kinetic experiments were performed at 20 °C. For determination of the rates of fluorescence-detected refolding of horse heart cytochrome *c*, a three-syringe SFM-3 (Bio-Logic) stopped-flow instrument was used. Cytochrome *c* in 3 M Gdn·HCl, pH 7.0, was diluted by mixing with 0.1 M sodium phosphate, pH 7.0, to give 0.2 M final concentration of Gdn·HCl and a final cytochrome *c* concentration of 10 μM. The fluorescence intensity at 350 nm was monitored at a right angle to the incident light (285 nm) through a 350-nm band-pass filter. For optimum detection of all three fluorescence-detected rate processes and their respective amplitudes, the signal was split, and data were collected simultaneously on two separately filtered time scales. The data were fit to functions with 1–3 exponential decay terms using software supplied by Bio-Logic.

The rate of combination of an antibody with a refolded epitope was determined by stopped-flow mixing by putting cytochrome *c* in 3.0 or 4.0 M Gdn·HCl, pH 7.0, in syringe number 1, 0.1 M sodium phosphate, pH 7.0, in syringe number 2, and antibody in sodium phosphate buffer in syringe number 3. Refolding of cytochrome *c* in the presence of antibody was initiated by dilution of Gdn·HCl with the buffer and the antibody solutions to give a final Gdn·HCl concentration of 0.2 M. A 0.8 × 0.8 × 10 mm fluorescence cuvette was used for the experiments. The final MAb/cytochrome *c* ratio was kept at 5.0 or greater so that the reaction occurred under pseudo-first-order conditions. MAb concentrations were kept very high (1–50 μM) so that the diffusion-limited rate of antibody association with the epitopes was as fast as possible. Epitope formation was monitored by fluorescence quenching of the antibody by the heme on complex formation with cytochrome *c*.

For 2B5 MAb, 2B5 FAb, and 5F8 MAb, respectively, the fluorescence changes on cytochrome *c* binding are 144-fold, 78-fold, and 105-fold larger than the intrinsic, kinetically resolved fluorescence changes for cytochrome *c* folding. We have been unable to detect intrinsic fluorescence changes from folding in our MAb-detected folding experiments because the intrinsic fluorescence changes from folding are so much smaller (~1%) than those for MAb–cytochrome *c* binding. Therefore, MAb binding can be monitored in the presence of protein folding without interference.

MAb–cytochrome *c* binding exhibits much larger changes in fluorescence than folding because of the large number of tryptophan residues in MAbs that are strongly quenched on cytochrome *c* binding. Compared to the fluorescence from an *N*-acetyltryptophanamide standard standard, the molar fluorescence at 350 nm from 2B5 MAb, 2B5 FAb, and 5F8 MAb is equivalent to that of 15.2, 7.7, and 21.1 tryptophan residues, respectively. Cytochrome *c* binding quenches these fluorescence signals to levels of 40%, 36%, and 69% of the initial fluorescence for 2B5 MAb, 2B5 FAb, and 5F8 MAb, respectively (Raman et al., 1992). In contrast, the total kinetically resolved fluorescence change for folding is equal to the fluorescence of only 0.063 tryptophan residue.

Absorbance-detected slow refolding of cytochrome *c* was performed by manual mixing experiments. The cytochrome *c* solution in 4 M Gdn·HCl, pH 7, was diluted with 0.1 M sodium phosphate buffer, resulting in a final concentration of 0.2 M Gdn·HCl and 4 μM cytochrome *c* at pH 7. Soret band absorbance measurements (418 nm, and 398 or 396 nm) were monitored over time in a 1-cm path-length cuvette using a Hewlett-Packard 8452A diode array spectrophotometer. To

improve base-line stability, absorbance measurements were made relative to the absorbance at 800 nm. Absorbance-detected refolding of cytochrome *c* in the presence of the antibodies was performed in the same manner except that the sodium phosphate dilution buffer contained antibody. For these experiments, the final antibody concentration was 5 μM (binding sites). The dead time for manual mixing experiments is estimated to be about 5 s. Data collected on the HP 8452A spectrophotometer were converted to the Biokine (Bio-Logic) file format by a format conversion program. The time course of the absorbance changes was fit to a first-order rate equation using the Biokine software.

Manual mixing experiments were also used to test whether the fluorescence-detected slow refolding intermediates contained refolded epitopes. These species account for ~12% of the kinetically detected change in fluorescence on refolding (Table 1). Cytochrome *c* in 4 M Gdn·HCl in 0.1 M sodium phosphate, pH 7.0, was diluted to 0.2 M Gdn·HCl by manual mixing with 0.1 M sodium phosphate, pH 7.0, containing MAb 2B5 or 5F8. A control mixing experiment was performed to determine the rate of association of MAb with the fully folded protein under refolding conditions. For the control experiments, cytochrome *c*, initially in the native conformation at 0.8 M Gdn·HCl, was diluted by stopped-flow mixing to the same final concentrations of cytochrome *c*, antibody, and Gdn·HCl as for refolding. Fluorescence intensity was measured at 350 nm as a function of time at a 90° angle to the 285-nm excitation light in a 1 cm × 1 cm cuvette using an SLM-500C spectrofluorometer. Mixing deadtimes of about 5 s are estimated for these experiments.

RESULTS

Antibodies 2B5 and 5F8 Bind to Native but Not Apocytochrome c. Antibodies used to monitor refolding must be specific for native epitopes and not bind to the unfolded protein. CD and NMR experiments indicate that when the heme of cytochrome *c* is removed, the protein adopts an unfolded, random-coil conformation under conditions where the holoprotein is native (Fisher et al., 1973; Stellwagen et al., 1972). Thus, apocytochrome *c* can be used as a model of the denatured state of the protein to test the specificity of cytochrome *c* antibodies. Antibodies with epitopes composed of linear sequences of amino acids (linear epitopes) will bind, presumably, to the denatured form of the protein and, perhaps, to the native protein as well. However, antibodies that recognize epitopes formed from distant segments of the protein that come together only in the folding process (tertiary or conformational epitopes) would, presumably, recognize only the native form of the protein antigen. ELISAs were performed to test the specificity of the antibodies. Both direct and competition ELISAs were performed. The direct ELISAs showed that neither the 2B5 MAb nor the 5F8 MAB bound to an ELISA plate coated with apocytochrome *c* (data not shown). A competition ELISA using the 2B5 MAb showed that addition of apocytochrome *c* to a solution of 2B5 MAb had no effect on the binding of the 2B5 MAb to an ELISA plate coated with native cytochrome *c* (data not shown). The results of the competition ELISA argue against the possibility that the direct ELISA was negative because of epitope denaturation on binding of the apoprotein to the ELISA plate. In addition, the competition ELISA tests for MAb–apocytochrome *c* interaction at known apocytochrome *c* concentrations that are comparable to the initial concentrations of unfolded cytochrome *c* in the MAb-detected refolding experiments. The results show that the antibodies do not bind apocytochrome *c*, but do bind to the native form of the protein. This suggests that both the 2B5 and 5F8 antibodies bind to tertiary epitopes found on the surface of the native protein.

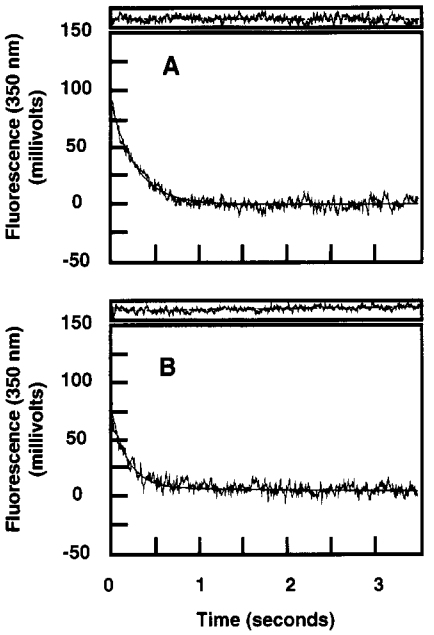

FIGURE 1: Refolding of cytochrome *c* detected by 2B5 MAb binding. MAb 2B5 binds native cytochrome *c* near a type II turn (residue 44). The rate of epitope refolding and MAb association is measured at final 2B5 MAb concentrations of (A) 13.3 μM binding sites and (B) 26.6 μM binding sites. Refolding is initiated by stopped-flow mixing in which unfolded cytochrome *c* in 3.0 M Gdn·HCl is mixed with dilution buffer containing the MAb to give final conditions of 0.2 M Gdn·HCl. The lines through the data are obtained as least-squares fits to a first-order rate equation with rate constants of (A) 3.5 s^{-1} and (B) 5.2 s^{-1}. The apparent increase in rate with increasing MAb concentration suggests that the bimolecular association reaction is rate-limiting rather than epitope-refolding. The rate of MAb–cytochrome *c* association in the absence of epitope refolding has been measured by mixing cytochrome *c* in 0.2 M Gdn·HCl with MAb in 0.2 M Gdn·HCl at an MAb concentration of 26.6 μM binding sites (data not shown). The rate constant of 6.3 s^{-1} is essentially the same as that obtained in (B) for refolding and association, verifying that the bimolecular association reaction is rate-limiting rather than epitope-refolding. For refolding and association (A, B) and association alone, the reactions are monitored by fluorescence quenching at 350 nm (285-nm excitation). The final fluorescence signal at equilibrium has been offset to zero. The upper panel shows the deviations of the data from a function obtained from a least-squares fit to a first-order rate equation. Other conditions are 0.1 M sodium phosphate, pH 7.0, 20 °C, and 2 μM cytochrome *c*.

MAb- and Fab-Detected Epitope Refolding. Measurement of the rate of refolding of an epitope requires that the diffusion-controlled rate of antibody binding to a fully formed epitope be faster than the rate of epitope formation from the unfolded protein. Under these conditions, refolding is rate-limiting, and the apparent rate of antibody–cytochrome *c* association will be independent of both antibody and cytochrome *c* concentration. Since antibody–epitope binding is a bimolecular reaction, the rate of association of antibody with a fully folded epitope will be proportional to the antibody concentration, so that the highest association rates occur at high antibody concentrations. In addition, by maintaining antibody concentrations at least 5-fold higher than the cytochrome *c* concentration, the association reaction is approximately first order, simplifying the data analysis. Nevertheless, even at high antibody concentrations we observe association rates that are proportional to antibody concentration, indicating that association rather than epitope refolding is rate-limiting. Compare the results in Figure 1A,B which

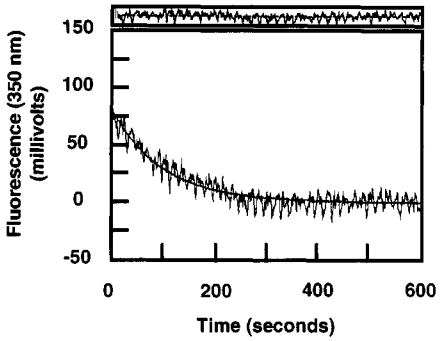

FIGURE 2: Refolding of cytochrome *c* detected by Fab fragments of monoclonal antibody 2B5. The rate of epitope refolding and Fab association is measured at a final 2B5 Fab concentration of 48 μM binding sites. Refolding is initiated by stopped-flow mixing in which unfolded cytochrome *c* in 4.0 M Gdn·HCl is mixed with dilution buffer containing Fab to give final conditions of 0.2 M Gdn·HCl. The line through the data is obtained from a least-squares fit to a first-order rate equation with a rate constant of 10.3 s^{-1}. The rate of Fab–cytochrome *c* association in the absence of epitope refolding has been measured by mixing cytochrome *c* in 0.2 M Gdn·HCl with Fab in 0.2 M Gdn·HCl at a Fab concentration of 48 μM binding sites (data not shown). The rate constant of 11.6 s^{-1} is essentially the same as that obtained for refolding and association, verifying that the bimolecular association reaction is rate-limiting. For refolding and association and association alone, the reactions are monitored by fluorescence quenching at 350 nm (285-nm excitation). The final equilibrium fluorescence signal has been offset to zero. Other conditions are 0.1 M sodium phosphate, pH 7.0, 20 °C, and 5 μM cytochrome *c*. The upper panel shows the deviations of the data from a function obtained from a least-squares fit to a first-order rate equation.

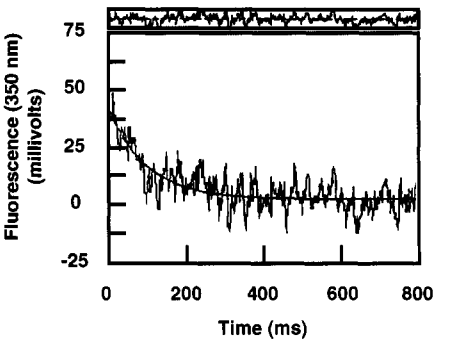

FIGURE 3: Refolding of cytochrome *c* detected by 5F8 MAb binding. MAb 5F8 binds native cytochrome *c* near the amino terminus of an α-helical segment (residue 60). The rate of epitope refolding and MAb association is measured at a final 5F8 MAb concentration of 20 μM binding sites. Refolding is initiated by stopped-flow mixing in which unfolded cytochrome *c* in 4.0 M Gdn·HCl is mixed with dilution buffer containing the MAb to give final conditions of 0.2 M Gdn·HCl and 2.5 μM cytochrome *c*. The line through the data is obtained from a least-squares fit to a first-order rate equation with a rate constant of 10.3 s^{-1}. The rate of MAb–cytochrome *c* association in the absence of epitope refolding has been measured by mixing cytochrome *c* in 0.2 M Gdn·HCl with MAb in 0.2 M Gdn·HCl to give final concentrations of 25 μM MAb binding sites and 5 μM cytochrome *c* (data not shown). The observed pseudo-first-order rate constant is 14.9 s^{-1}. Correction of this rate constant to the lower MAb concentration used for MAb-detected folding gives a pseudo-first-order rate of 11.9 s^{-1}, which is that expected if association is rate-limiting rather than epitope-refolding. For refolding and association and association alone, the reactions are monitored by fluorescence quenching at 350 nm (285-nm excitation). The final equilibrium fluorescence signal has been offset to zero. Other conditions are 0.1 M sodium phosphate, pH 7.0, and 20 °C. The upper panel shows the deviations of the data from a function obtained from a least-squares fit to a first-order rate equation.

show the effects of a 2-fold increase in the concentration of antibody 2B5 on the apparent rate of antibody-detected refolding of the 2B5 epitope. At an antibody concentration of 13.3 μM binding sites (Figure 1A), the apparent rate constant for association with the refolding protein is 3.5 s^{-1}, but at 26.6 μM binding sites (Figure 1B), the apparent pseudo-first-order rate increases to 5.2 s^{-1}. As a further test of whether the association reaction was rate-limiting, the rates of antibody–epitope association were measured directly in the absence of refolding by mixing antibody with native cytochrome *c*. At 13.3 μM antibody binding sites, the pseudo-first-order association rate was 3.7 s^{-1}, and at 26.6 μM antibody sites, the rate was 6.3 s^{-1} (data not shown). Since the association reactions have the same rates as refolding and association, we conclude that association is rate-limiting rather than epitope formation. Ideally, the concentration of antibody could be increased further until the bimolecular association reaction was faster than the rate of epitope refolding. Unfortunately, experiments with significantly higher antibody concentrations are not possible due to technical problems associated with fluorescence inner filter effects.

Somewhat higher concentrations of antibody binding sites can be used with Fab fragments rather than intact antibodies since Fab fragments have a lower absorbance per binding site equivalent. Fab-detected refolding of cytochrome *c* was possible at an almost 2-fold higher binding site concentration than for intact MAb molecules. Figure 2 shows the kinetics of Fab 2B5 binding to refolding cytochrome *c* at a final concentration of 48 μM Fab binding sites. The pseudo-first-order rate was 10.3 s^{-1}. The control reaction in which the association rate is measured under identical conditions but in the absence of refolding gave a rate of 11.6 s^{-1} (data not shown). These results indicate that the association reaction remains rate-limiting, even for Fab-detected refolding. Thus, a rate of 10.3 s^{-1} is a lower limit for the rate of epitope 2B5 formation in refolding.

Similar data have been obtained with antibody 5F8 which binds native cytochrome *c* near residue 60. At antibody binding site concentrations of 20 μM, the pseudo-first-order rate constant for folding and association is 10.3 s^{-1} (Figure 3). At similar antibody and cytochrome *c* concentrations, the association reaction alone has about the same rate as refolding and association, indicating that the overall reaction is rate-limited by antibody–epitope association, rather than by epitope refolding (data not shown). Thus, the rate of 10.3 s^{-1} is a lower limit for the rate of epitope 5F8 formation in refolding.

Optically-Detected Cytochrome c Refolding. The rate of cytochrome *c* refolding has been measured by intrinsic (cytochrome *c*) fluorescence changes under conditions identical to those used to monitor refolding by antibody binding. Figure 4A,B shows the fluorescence-detected refolding of cytochrome *c* following a 3 to 0.2 M Gdn·HCl concentration jump. The signal change on refolding is from quenching of the fluorescence from the single tryptophan residue by the heme as the protein refolds (Tsong, 1974). Under the conditions of the experiment, cytochrome *c* has three fluorescence-detected phases with apparent rate constants of k_1 = 4.9 s^{-1}, k_2 = 0.43 s^{-1}, and k_3 = 0.037 s^{-1} (Figure 4A,B). The fraction of the total fluorescence change associated with each phase is given in Table 1. Since the kinetically observed change in fluorescence is smaller than the fluorescence change observed in an equilibrium unfolding experiment, an unresolved kinetic phase, k_0, is postulated to account for the missing fluorescence. Since phase k_0 is not detected directly, it may involve more than one kinetic event. The slowest phase, k_3, is thought to result from unfolded species of cytochrome *c* with one or more proline residues in the *cis* conformation (Brandts et al., 1975; Brems & Stellwagen, 1983). Before folding can go to completion, the *cis* proline residues in these species must

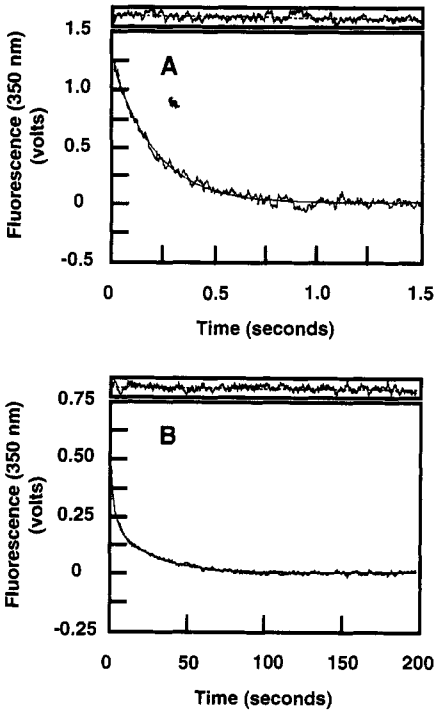

FIGURE 4: Fluorescence-detected refolding of cytochrome *c*. Refolding was initiated by a 15-fold dilution of cytochrome *c* in 3.0 M Gdn·HCl to give final concentrations of 10 μM cytochrome *c* and 0.2 M Gdn·HCl. Fluorescence quenching of the single tryptophan residue in cytochrome *c* was monitored at 350 nm (285-nm excitation). In the fast time range (A), the signal was filtered using an 8-ms time constant and fit to a single-exponential decay curve with $k_1 = 4.8$ s^{-1}. For the slower time range (B), the signal was filtered using a 330-ms time constant and fit to a decay curve consisting of the sum of two exponential terms with $k_2 = 0.43$ s^{-1} and $k_3 = 0.037$ s^{-1}. Other conditions are 0.1 M sodium phosphate, pH 7.0, and 20 °C. Upper panels show deviations of the data from functions obtained from least-squares fits to decay curves consisting of one (A) or two (B) exponential terms. The final equilibrium fluorescence signal has been offset to zero.

isomerize to the native *trans* isomeric state in an intrinsically slow reaction. Refolding has also been monitored by Soret absorbance changes. The kinetic phases and associated amplitudes are listed in Table 1.

Taken together with the Fab binding and MAb binding experiments, these experiments show that the rate of refolding of both epitopes of horse cytochrome *c* is at least as fast, and probably faster, than the fastest absorbance- or fluorescence-detected phases in refolding of cytochrome *c*.

Slow Folding Reactions. The slow kinetic phases in refolding of cytochrome *c* are believed to arise from the presence of nonnative proline isomers in the unfolded protein. There is evidence that many unfolded species are rapidly converted to highly structured intermediate species prior to slow isomerization or other reactions that yield the fully native protein (Elove et al., 1992). Manual mixing experiments were performed to determine whether the epitopes for the 5F8 and 2B5 antibodies were present in rapidly formed structured folding intermediates, or whether epitope formation occurs only after a slow isomerization of these species to the fully native protein in the slow folding phase. Concentrations of antibody and cytochrome *c* were chosen so that the bimolecular rate of association of antibody with cytochrome *c* occurred within the dead time (~5 s) of the manual mixing experiment. Thus, there should be no detectable kinetic phase if epitopes are already present on the slow refolding intermediate species. If, on the other hand, the epitopes are formed slowly in an isomerization-requiring reaction, then a slow phase should be observed with the antibody binding assay. The manual mixing experiments show that there is no detectable fluorescence change for refolding in the presence of antibody 2B5 or 5F8 on a slow time scale (data not shown), indicating that the epitopes have already formed in the structured slow folding intermediates. The intrinsic changes in cytochrome *c* fluorescence on refolding can be ignored in this experiment since they are negligible compared to the fluorescence changes for antibody–cytochrome *c* complex formation (see Materials and Methods).

Absorbance-Detected Slow Folding of Free and Antibody-Bound Cytochrome c. When an antibody binds to a folding intermediate, the additional steps in folding of the protein may be perturbed by the binding process. Measurements of the rates of slow steps in folding that follow MAb binding provide a test of whether MAb binding perturbs subsequent folding reactions. For fluorescence-detected folding, this is technically difficult since the fluorescence changes on antibody–cytochrome *c* association are very large and mask the folding-associated changes in cytochrome *c* fluorescence (see Materials and Methods). In contrast, measurements of subsequent folding by heme absorbance are relatively easy since there are no significant changes in heme absorbance for the MAb–cytochrome *c* association reaction (Raman et al., 1992). Figure 5A shows the kinetics of refolding of cytochrome *c* at 418 nm in the time range of the slowest absorbance-detected kinetic phase. This kinetic phase probably results from the small population of cytochrome *c* with one or more prolines in the nonnative (*cis*) configuration. The absorbance at 418 nm increases during refolding. The rate constant for slow absorbance-detected refolding is 0.03 s^{-1} in the absence of antibody. When antibody 2B5 is bound to rapidly formed folding intermediates of cytochrome *c*, the slow refolding process has the same rate as in the absence of antibody (Figure 5B). Similarly, binding of antibody 5F8 to a folding

Table 1: Kinetic Parameters for Cytochrome *c* Refolding[a]

probe	a_0	k_0 (s^{-1})	a_1	k_1 (s^{-1})	a_2	k_2 (s^{-1})	a_3	k_3 (s^{-1})
cyt *c* fluorescence[b]	0.79	>100	0.14 (0.66)	4.9 ± 0.7	0.046 (0.22)	0.43 ● 0.11	0.025 (0.12)	0.037 ± 0.004
cyt *c* heme absorbance[c]	0.19	>100	0.53 (0.65)	4.7 ± 1.5	0.16 (0.20)	0.29 ± 0.06	0.12 (0.15)	0.027 ± 0.004
MAb/Fab 2B5 binding[d]	1.0	>10	0		0		0	
MAb 5F8 binding[d]	1.0	>10	0		0		0	

[a] Cytochrome *c* unfolded in 3–4 M Gdn·HCl is induced to refold by dilution of the denaturant to 0.2 M Gdn·HCl by stopped-flow mixing. Other conditions are 0.1 M sodium phosphate, pH 7.0, 20 °C. The kinetic parameters a_i and k_i are the amplitudes and apparent rate constants, respectively, obtained by fitting the kinetic data to functions of the form: $S(t) = \sum_i a_i e^{-k_i t}$, where $S(t)$ is the signal at time t. The parameters a_0 and k_0 are the amplitude and limiting rate, respectively, for unresolved kinetic processes occurring within the dead time of the mixing experiments. The relative amplitudes of the kinetically resolved phases in folding are given in parentheses. Errors in the rate constants have been estimated from the standard deviations of three or more independent measurements. [b] Fluorescence of Trp-59 in cytochrome *c* is measured at 350 nm with excitation at 285 nm. [c] Heme absorbance changes are measured at 396 and 418 nm, shoulders of the Soret absorbance maximum. [d] MAb 2b5 binds to cytochrome *c* near a type II turn (amino acid residue 44) while MAb 5F8 binds to a distinct epitope near the amino terminus of an α-helical segment of the protein (amino acid residue 60). Presumably, each of these antibodies is a site-specific probe of folding in the neighborhood of their respective epitopes.

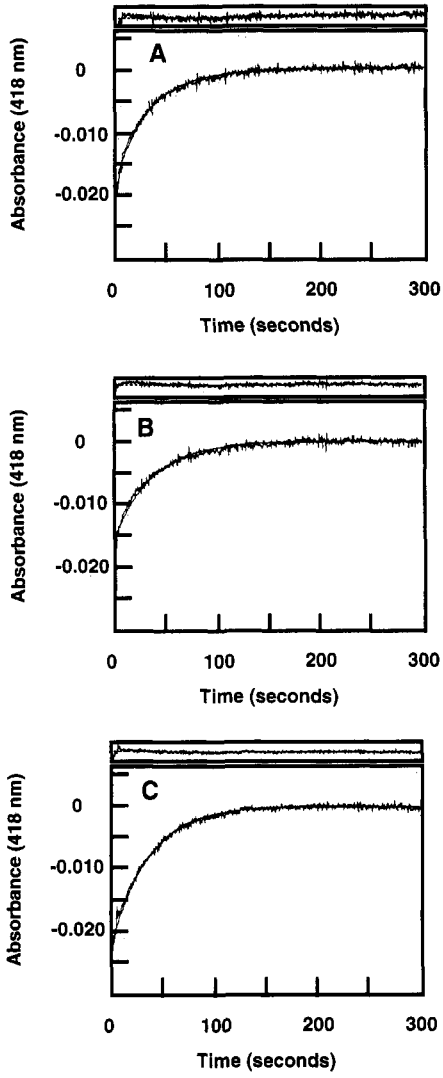

FIGURE 5: Comparison of rates for absorbance-detected slow folding of cytochrome *c* in the presence and absence of the 2B5 and 5F8 MAbs. For refolding in the presence of the MAbs, the MAb–cytochrome *c* association reaction goes to completion within the mixing dead time of the experiment, so the observed kinetic changes are for refolding of a folding intermediate in complex with an MAb (see Discussion). Refolding was initiated by mixing cytochrome *c* in 4.0 M Gdn·HCl with buffer to give final refolding conditions of 0.2 M Gdn·HCl and 4 μM cytochrome *c*. Data are shown in the slow refolding time range for refolding of cytochrome *c* alone (A), refolding of cytochrome *c* in the presence of 4.4 μM of the 2B5 MAb (B), and refolding of cytochrome *c* in the presence of 4.3 μM of the 5F8 MAb (C). The absorbance changes at 418 nm were monitored over time in a 1-cm path-length cuvette. To improve long-term base-line stability, the absorbance changes at 800 nm (largely due to instrumental fluctuations) were subtracted for those at 418 nm before data analysis. The lines through the data were obtained from least-squares fits to a first-order rate equation using a simplex routine provided by Biologic. The rate constants (k_3) are 0.03 s^{-1} in the absence of MAb (A), 0.027 s^{-1} in the presence of MAb 2B5 (B), and 0.027 s^{-1} in the presence of MAb 5F8 (C). Other conditions are 0.1 M sodium phosphate, pH 7.0, and 20 °C. Upper panels show the deviations of the data from a first-order rate expression obtained by least-squares fitting. The final equilibrium absorbance signal has been offset to zero.

intermediate does not change the rate for the absorbance-detected slow refolding reaction (Figure 5C).

DISCUSSION

Major Changes in Fluorescence Occur Prior to Kinetically Resolved Phases in Folding. The results show (Table 1) that 79% of the total change in fluorescence occurs within the 4–6-ms mixing dead time of the stopped-flow experiments. Three kinetic phases account for the remaining 21% of the total change in fluorescence observed in equilibrium unfolding experiments. Large, kinetically unresolved changes in fluorescence have been reported previously by Elove et al. (1992) for folding of horse cytochrome *c* and by Nall (1983) for folding of yeast iso-2 cytochrome *c*. The rapid changes in fluorescence indicate formation of a structure which decreases the heme to Trp-59 distance and results in enhanced tryptophan fluorescence quenching (Tsong, 1974). Differences between our results for fluorescence-detected refolding of horse cytochrome *c* and those of Elove et al. (1992) are as follows: (1) we observe an additional slow phase in folding ($k_3 = 0.037$ s^{-1}, Table 1); (2) we fail to detect the fastest kinetic phase they report ($k = 56$ s^{-1}); (3) we find that a larger fraction (79% versus 35%) of the fluorescence change is too fast to detect by stopped-flow mixing. The most likely explanation for the different results is that somewhat different conditions were used for the refolding experiments (see below).

Epitope Refolding Precedes Folding of Fluorescence/Absorbance-Detected Species. The results (Table 1; Figures 1–4) show that the rates of refolding of the epitopes corresponding to the 2B5 and 5F8 antibodies are at least as fast, and probably faster, than the fastest kinetically resolved fluorescence-detected refolding phase for cytochrome *c*. Rapid re-formation of surface epitopes is in qualitative accord with the conclusions of others, who have used stopped-flow mixing together with H–D pulse labeling, or circular dichroism, to monitor refolding of cytochrome *c* (Elove et al., 1992; Roder et al., 1988). These alternative probes of folding indicate formation of significant amounts of secondary structure prior to the absorbance-detected or fluorescence-detected kinetic phases in folding (Elove et al., 1992). The H–D pulse labeling studies suggest that much of the stable H-bonding in both the N- and C-terminal helices forms on a ~10–20-ms time scale, indicating that intramolecular association of the N- and C-terminal helices may be the factor stabilizing the H-bonds in the N- and C-terminal α-helices.

The results indicate that substantial refolding takes place within the dead times of stopped-flow mixing and the (diffusion-limited) MAb-detected folding techniques. These kinetically unresolved folding reactions yield incompletely folded intermediate species as products. These species contain MAb binding-competent epitopes but have neither the spectral features nor the reducibility of the native protein. In contrast, refolding detected by absorbance changes (695 nm) has been shown to yield native cytochrome *c* as a product of both the fast and slow kinetically resolved phases in folding. Soret absorbance (405 nm) and ascorbate reducibility detect folding reactions in time ranges similar to those detected by 695-nm absorbance, but these probes also indicate the presence of folding intermediates on both the fast and slow time ranges (Ridge et al., 1981). While the kinetically unresolved changes in fluorescence and MAb binding indicate substantial rapid structure formation early on, completion of folding to yield the fully native protein occurs in kinetically resolved phases in folding.

Are Folded 2B5 and 5F8 Epitopes a General Structural Feature of All Species Present Early in Folding? MAb-detected folding indicates that structure recognizable by antibodies forms within the first ~100 ms of folding ($k_{app} > 10$ s^{-1}) and, moreover, that this structure forms in *all* of the species present. In contrast only 60–77% of the secondary structure is formed in the initial stages of folding ($k_{app} > 10$ s^{-1}). The remainder of the secondary structure is regained or

stabilized in additional slow kinetic phases (Elove et al., 1992; Roder et al., 1988). Thus, refolded 2B5 and 5F8 epitopes are a common feature of the structure of early folding intermediates that differ in other aspects of their structure. Compared to many other probes of refolding, MAb-detected folding provides a more homogeneous view of early folding intermediates. Soon after initiation of folding there is sufficient structure formation for MAb binding. In contrast, absorbance, near-UV CD, fluorescence, and H–D pulse labeling indicate a heterogeneous population of refolding molecules with distinct spectral and hydrogen exchange properties (Elove et al., 1992; Roder et al., 1988). The properties of these species return to those of the fully native protein in kinetically resolved phases in folding (Ridge et al., 1981). Much of the kinetic heterogeneity in protein refolding is known to result from a heterogeneous unfolded state (Garel & Baldwin, 1973) in which kinetically distinguishable unfolded species differ in the *cis* or *trans* isomeric states of proline imide bonds (Brandts et al., 1975). Apparently, refolding of both the 2B5 and 5F8 epitopes proceeds despite the presence of nonnative proline isomers and, perhaps, other forms of structural heterogeneity among the refolding species.

In comparing our results to those of Elove et al., it is important to note that the final refolding conditions vary somewhat: 20 °C and 0.2 M Gdn·HCl for our experiments vs 10 °C and 0.7 M Gdn·HCl for those of Elove et al. (Elove et al., 1992; Roder et al., 1988). We have carried out fluorescence-detected refolding experiments at higher guanidine hydrochloride concentrations and lower temperatures that show that the fastest kinetically resolved phase under our conditions (k_1 in Table 1) corresponds to the second fastest kinetically resolved phase of Elove et al. [k_2 in Table 1 of Elove et al. (1992)]. Our results show that epitope formation has gone to completion in 100% of the refolding molecules within the first ~100 ms of folding, and suggest that MAb binding competence is one aspect of the structure of at least some of the intermediates detected by H–D pulse labeling or CD measurements of refolding.

Do Epitopes Preexist in Folding Intermediates or Are They Induced by MAb Binding? While the structural integrity of the epitopes recognized early in refolding is unknown, epitope structure in the folding intermediates is adequate for binding by either the 2B5 or the 5F8 MAb with the *same* diffusion-controlled association rate constants as for binding to epitopes on the native protein (Raman et al., 1992). This suggests that substantial epitope structure is present in the fast folding intermediates prior to MAb binding. The MAb binding process may induce additional structural changes in partially formed epitopes and, thus, enhance the equilibrium binding affinity. If so, the structure-inducing step(s) would enhance the binding equilibrium constant primarily by slowing the off rate while the on rate remained unchanged at the diffusion-controlled limit [see Friguet et al. (1989)]. The results show that the folding intermediates responsible for the absorbance-detected slow folding phase also contain binding-competent 2B5 and 5F8 epitopes. Again, MAb binding may induce further structural change and/or stabilize the epitope structure within the slow folding intermediates. If they occur, binding-induced changes in epitope structure or stability do not affect kinetic processes occurring within the absorbance-detected slow folding phase, since the rate of the absorbance-detected slow folding reaction is not affected by MAb binding (Figure 5). This places some rather severe limitations on the kinds of structural rearrangements that can occur in attaining and traversing the transition state for absorbance-detected slow folding.

ACKNOWLEDGMENT

We are grateful to Sudha Veeraragahaven for providing comments on an early draft of the manuscript and for writing the computer program used to convert kinetic data obtained on the Hewlett-Packard UV–visible spectrophotometer to the Biokine format. C. S. Raman is thanked for help with the competitive ELISAs. We are grateful to Michel Goldberg (Institut Pasteur) for an enlightening discussion and for detailed comments on the manuscript.

REFERENCES

Baldwin, R. L., & Roder, H. (1991) *Curr. Biol. 1*, 218–220.
Blond-Elguindi, S., & Goldberg, M. E. (1990) *Biochemistry 29*, 2409–2417.
Brandts, J. F., Halvorson, H. R., & Brennan, M. (1975) *Biochemistry 14*, 4953–4963.
Brems, D. N., & Stellwagen, E. (1983) *J. Biol. Chem. 258*, 3655–3660.
Elove, G. A., Chaffotte, A. F., Roder, H., & Goldberg, M. E. (1992) *Biochemistry 31*, 6876–6883.
Fisher, W. R., Taniuchi, H., & Anfinsen, C. B. (1973) *J. Biol. Chem. 248*, 3188–3195.
Friguet, B., Djavadi-Ohaniance, L., & Goldberg, M. (1989) *Res. Immunol. 140*, 355–376.
Garel, J. R., & Baldwin, R. L. (1973) *Proc. Natl. Acad. Sci. U.S.A. 70*, 3347–3351.
Goshorn, S. C., Retzel, E., & Jemmerson, R. (1991) *J. Biol. Chem. 266*, 2134–2142.
Murry-Brelier, A., & Goldberg, M. E. (1988) *Biochemistry 27*, 7633–7640.
Nall, B. T. (1983) *Biochemistry 22*, 1423–1429.
Raman, C. S., Jemmerson, R., Nall, B. T., & Allen, M. J. (1992) *Biochemistry 31*, 10370–10379.
Ridge, J. A., Baldwin, R. L., & Labhardt, A. M. (1981) *Biochemistry 20*, 1622–1630.
Roder, H., & Wuthrich, K. (1986) *Proteins: Struct., Funct., Genet. 1*, 34–42.
Roder, H., Elove, G. A., & Englander, S. W. (1988) *Nature 335*, 700–704.
Stellwagen, E., Rysavy, R., & Babul, G. (1972) *J. Biol. Chem. 247*, 8074–8077.
Tsong, T. Y. (1974) *J. Biol. Chem. 249*, 1988–1990.
Udgaonkar, J. B., & Baldwin, R. L. (1988) *Nature 335*, 694–699.